


## Quantitative phase imaging via the holomorphic property of complex optical fields

Jeonghun Oh <sup>1,2</sup>, Herve Hugonnet,<sup>1,2</sup> and YongKeun Park <sup>1,2,3,\*</sup>

<sup>1</sup>*Department of Physics, Korea Advanced Institute of Science and Technology (KAIST), Daejeon 34141, Republic of Korea*

<sup>2</sup>*KAIST Institute for Health Science and Technology, Korea Advanced Institute of Science and Technology, Daejeon 34141, Republic of Korea*

<sup>3</sup>*Tomocube Inc., Daejeon 34109, Republic of Korea*



(Received 29 August 2022; accepted 13 March 2023; published 18 April 2023)

An optical field is described by the amplitude and phase, and thus has a complex representation described in the complex plane. However, because the only thing we can measure is the amplitude of the complex field on the real axis when not introducing an additional imaging system, it is difficult to identify how the complex field behaves throughout the complex plane. In this study, we interpret quantitative phase imaging methods via the Hilbert transform in terms of analytic continuation, manifesting the behavior in the whole complex plane. Using Rouché's theorem, we prove the imaging conditions imposed by Kramers-Kronig holographic imaging. The deviation from Kramers-Kronig holography conditions is examined using computational images and experimental data. We believe that this study provides a clue for holographic imaging using the holomorphic characteristics of a complex optical field.

DOI: [10.1103/PhysRevResearch.5.L022014](https://doi.org/10.1103/PhysRevResearch.5.L022014)

### I. INTRODUCTION

Holography retrieves the amplitude and phase of a light field, which has been recently exploited for various applications of quantitative phase imaging (QPI). The obtained field is related to the material thickness and refractive index (RI), allowing the imaging of highly transparent objects. Holographic measurements have been utilized in various fields such as rheology [1], nanotechnology [2], biological science [3–6], microfluidics [7–9], and metrology [10,11]. Unfortunately, when an optical imaging sensor is used without a special imaging system, it is only possible to directly measure the intensity of the light fields in the IR, visible, UV, or shorter wavelength regions due to the limited temporal bandwidth of an electronic device. The problem of retrieving the phase from the magnitude information is significantly difficult and historical, known as the *phase problem* [12–14].

With the application of QPI in the biomedical field [15–19], there have been remarkable developments in holographic imaging methods for the reconstruction of complex fields. The retrieval of a complex field falls mainly into two categories: recovering the analytic form of an optical field [20–22] or approaching the correct solution by employing an iterative algorithm [23–25]. There are two approaches for obtaining an analytic solution in terms of methodology: using a reference arm [26,27] or in the noninterferometric regime [28,29]. The complete reconstruction of a complex field

without an iterative method not only increases the efficiency of imaging but also eliminates concerns about the possibility of convergence to a correct solution [30]. However, finding an analytical solution with only one intensity image without the assistance of a reference field is challenging. For example, the approach using the transport intensity equation [31,32] provides an elegant way to reconstruct the phase of a complex field by solving a partial differential equation, but requires at least two intensity images and is not capable of imaging all complex optical fields accurately.

Recently, a phase-retrieval algorithm using Kramers-Kronig (KK) relations was proposed [33,34]. When a complex field is analytic and square integrable in the upper half plane (UHP) of the complex plane, the real and imaginary parts of the field are related through the Hilbert transform of each other, which is called the KK relation. Although attempts to conduct phase retrieval using the properties of a complex analytic field were made extensively in the 1970s and the 1980s [35–38], holographic imaging via the KK relations was applied experimentally only recently [33,39–43].

This study investigates the analyticity of an optical field, focusing on holographic imaging, and describes the significance of analyticity in the one-dimensional (1D) phase problem following a procedure similar to that in Ref. [22]. The approach using a Hilbert transform is based on the 1D phase problem because each line of the measured intensity distribution is considered to be the real axis in a complex plane; KK holographic imaging reconstructs phase information through integration on the real axis. Higher-dimensionality images can also be analyzed in the 1D regime by considering each line along a given direction independently. Approaches via complex analysis for the two-dimensional phase problem are possible but more complicated because it is necessary to consider a hyperplane in which two complex planes are conjugated [44,45].

\*yk.park@kaist.ac.kr

Published by the American Physical Society under the terms of the [Creative Commons Attribution 4.0 International](https://creativecommons.org/licenses/by/4.0/) license. Further distribution of this work must maintain attribution to the author(s) and the published article's title, journal citation, and DOI.

We aim to provide a comprehensive description of holographic imaging exploiting analyticity. The principle of imaging performed using the Hilbert transform is mathematically interpreted using Hilbert microscopy [46] and KK holography [33]. We prove the conditions that make KK holographic imaging hold in terms of complex analysis. The situation in which the conditions of KK holography are not satisfied is also examined using simulation and experimental data.

## II. THEORY AND RESULTS

### A. Holomorphic complex optical field

For a complex function  $f(z)$ , it is said to be analytic at  $z = z_0$  if the function is complexly differentiable at all points in the neighborhood of  $z = z_0$ . To avoid confusion with the literal meaning or different usages of the word analytic for real functions, in this study, the analyticity of complex functions is expressed as *holomorphic*; a complex function is holomorphic in a domain or the whole complex plane if the function is analytic at all points in the domain or the complex plane [47].

One can see from the Paley-Wiener theorem that most complex optical functions in imaging systems are holomorphic. The Paley-Wiener theorem [48–51] states that if a function  $F(u)$  is supported in  $[-C, C]$ , its complex inverse Fourier transform from  $\mathbb{R}$  (set of real numbers) to  $\mathbb{C}$  (set of complex numbers)

$$f(z) = \int_{-C}^C F(u) e^{iuz} du \quad (1)$$

is an entire function of exponential type  $C$ , which means that it is holomorphic. The fact that such a function is holomorphic can be understood from the Cauchy-Riemann equations in Eq. (1) respects Ref. [47]:

$$\frac{\partial \text{Re}[f(z)]}{\partial x} = \frac{\partial \text{Im}[f(z)]}{\partial y}. \quad (2)$$

When an objective lens is used in an imaging system, the Fourier spectrum is limited by the numerical aperture (NA) of the lens, as shown in Figs. 1(a) and 1(b). According to the Paley-Wiener theorem, these complex fields are said to be bandlimited and become holomorphic functions. The most complex optical fields in imaging systems have a holomorphic nature. If the 1D regime is considered, the value of  $C$  is  $2\pi(\text{NA})/\lambda$ , where  $\lambda$  is the wavelength.

Equation (1) can be used to obtain a complex function  $f(z)$  that matches the value of a real variable function  $f(x)$  on the real axis:

$$f(x + iy_0) = \int_{-C}^C F(u) e^{iux} e^{-uy_0} du = \mathcal{F}_{\text{1D}}^{-1}[F(u) e^{-iy_0}], \quad (3)$$

with  $F(u) = \mathcal{F}_{\text{1D}}[f(x)]$ , where  $\mathcal{F}_{\text{1D}}$  represents a 1D Fourier transform. For example,  $\sin z$  is the only function whose value on the real axis is the same as  $\sin x$ , reflecting the identity theorem [52]. This redefinition of a function by extending a domain, such as from  $f(x)$  to  $f(z)$  [Figs. 1(c) and 1(d)], is called analytic continuation in mathematics [53–55].

### B. Complex analysis as a tool for retrieving phase information

The KK relations associate the imaginary part with the real part of a complex function  $f(z)$  that is holomorphic in the

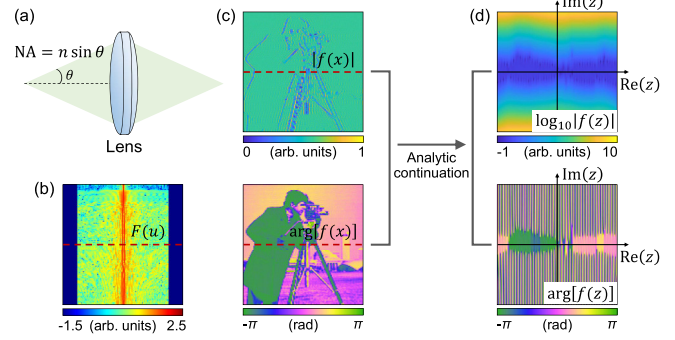


FIG. 1. Holomorphic  $E$ -field analytic in the whole complex plane. (a) Imaging system with a lens that limits the Fourier spectrum of a sample as the NA.  $n$  is the RI of a surrounding medium. (b) Amplitude (log scale) of the 1D Fourier transform of a sample field. The Fourier spectrum is supported along with the indicated direction. (c) Amplitude and phase of a sample field. Each line in the direction of the indicated arrow represents the real axis in some complex plane, respectively. (d) Amplitude (log scale) and phase of a complex field expanded to the whole complex plane by analytic continuation. Red dotted lines in (b) and (c) correspond to the function value on a real axis  $f(x)$  expanded to the function value in the whole complex plane  $f(z)$  in (d) and its 1D Fourier transform  $F(u)$ .

UHP and vanishes at infinity in the UHP [56,57]:

$$\begin{aligned} \text{Im}[f(x)] &= -\frac{1}{\pi} \text{p.v.} \int_{-\infty}^{\infty} \frac{\text{Re}[f(x')]}{x' - x} dx' \\ \text{Re}[f(x)] &= \frac{1}{\pi} \text{p.v.} \int_{-\infty}^{\infty} \frac{\text{Im}[f(x')]}{x' - x} dx' \end{aligned} \quad (4)$$

where p.v. is the Cauchy principal value. The KK relations are often derived using contour integration [58], which is why  $f(z)$  vanishes at infinity. The vanishing condition is equivalently expressed using Titchmarsh's theorem [48,59,60] as the Fourier transform of a complex function that needs to be supported on a positive frequency in  $[C_{\text{min}}, C_{\text{max}}]$ , where  $C_{\text{max}} > C_{\text{min}} > 0$ . This condition can be understood from the fact that the negative spatial frequencies in Eq. (1) go to infinity as  $\text{Im}(z)$  goes to infinity, thus not reflecting the vanishing condition. This holomorphic property is ensured by the Paley-Wiener theorem. In conclusion, the KK relations can be applied to any bandlimited signal with only positive spatial frequencies.

An important application of the KK relations is the retrieval of a complex field from its modulus because many rapidly oscillating quantities in physics, such as light, can only be measured by their modulus in the optical regime. In this case, instead of applying the KK relations to the real part of a complex signal, the real part of the logarithm of a signal can be subject to the KK relations, as follows:

$$\begin{aligned} g(z) &= \log[1 + f(z)], \\ \text{Re}[g(z)] &= \log|1 + f(z)|, \\ \text{Im}[g(z)] &= \arg(1 + f(z)), \end{aligned} \quad (5)$$

where  $f(z)$  only has positive spatial frequencies. This complex logarithm  $g(z)$  is holomorphic if  $f(z)$  is holomorphic and  $1 + f(z)$  does not vanish in the UHP [61]. This proposition

can be intuitively understood.  $\log f$  at the zeros of  $f$  is not only undefined but also nonanalytic;  $\log f$  is also not square integrable because  $\log f$  diverges to infinity at the zeros of  $f$ .

Whether  $1 + f(z)$  vanishes in the UHP can be checked from its value on the real axis using  $|f(x)| < 1$ ,  $x \in \mathbb{R}$ , and the fact that  $f(z)$  is holomorphic and vanishes at infinity. Rouché’s theorem [52,60] bestows a mathematical rationale for the behavior of zeros of a complex function: for two complex functions  $f_1(z)$  and  $f_2(z)$  holomorphic inside some region  $D$  with closed contour  $\partial D$ , if  $|f_1(z)| > |f_2(z)|$  on  $\partial D$ , then  $f_1$  and  $f_1 + f_2$  have the same number of zeros inside  $D$ , where each zero is counted as many times as its multiplicity. If  $f_1 = 1$ ,  $f_2 = f(z)$ , and  $D$  are set to a large domain in the UHP including the real axis, Rouché’s theorem ensures that  $1 + f(z)$  has no zeros in the UHP because  $f(z)$  vanishes at infinity in the UHP. Hence,  $g(z) = \log[1 + f(z)]$  is holomorphic in the UHP if  $|f(x)| < 1$  and  $x \in \mathbb{R}$ .

Finally,  $g(z)$  also vanishes at infinity because the Taylor series of  $g(z)$  is expressed as a series with no zero-order coefficient, and the powers of  $f(z)$  vanish at infinity in the UHP,

$$g(z) = \log[1 + f(z)] = \sum_{n=0}^{\infty} \frac{(-1)^n}{n+1} [f(z)]^{n+1}. \quad (6)$$

Note that from the holomorphic property of  $g(z)$ , the Taylor series of  $g(z)$  converges to  $g(z)$  in the UHP.

In summary, the KK relations can be used on the logarithm of a complex function if the function is supported on a closed set of positive frequencies in Fourier space and is of a norm smaller than 1. If a complex field has no zero in the UHP, its logarithm can be reconstructed accurately via a Hilbert transform [37]. The presented proof borrows tools from complex analysis to derive the conditions of KK holographic imaging. In the process of retrieving a complex field through the KK relations, it can be seen that the growth condition is more decisive than the analytic condition. Furthermore, zeros may be removed to take advantage of phase retrieval using a Hilbert transform. Rouché’s theorem can be used to eliminate zeros in the UHP.

We can further consider a more general situation, in which a complex function has zeros in the UHP. If  $f(z)$  has negative spatial frequencies, or  $|f(x)| < 1$  is not satisfied for all  $x$ ,  $1 + f(z)$  may have zeros in the UHP so that the KK relations do not hold. In these cases, a holomorphic function of exponential type can be represented by its zeros [38,49]. In particular, such a function is expressed by the Hilbert transform of the logarithm of the magnitude and the location of the complex zeros in the UHP [62–64]. When the function satisfies some growth and boundedness conditions, the following equation holds:

$$f(x) = m|f(x)|B(x) \exp(i\mathcal{H}[\log|f(x)|]), \quad (7)$$

where

$$B(x) \equiv \prod_j \frac{z_j - x}{z_j^* - x}, \quad (8)$$

called the Blaschke product [62],  $m$  is a constant of modulus 1,  $\{z_j\}$  denotes the sequence of zeros, and  $*$  and  $\mathcal{H}$  stand for the complex conjugate and a Hilbert transform, respectively.

Function values other than the real axis are expanded using analytic continuation. This equation extends the potential of phase retrieval via a Hilbert transform by considering the case when the conditions of KK holographic imaging do not hold. For example, in Ref. [65], the authors reconstruct the phase information of the field induced by a point dipole inside a cavity using modified KK relations with the calculation of the Blaschke product.

It should be emphasized that we can only measure the magnitude of a complex field on the real axis, that is,  $|f(x)|$ . The sequence of the complex conjugate of zeros,  $\{z_j^*\}$ , also yields the same magnitude but different complex values of  $f(x)$  according to Eq. (7). This ambiguity of zeros is the fundamental origin of the inability to uniquely determine a solution to the 1D phase problem, known as zero flipping [45].

### C. Interpretation of QPI methods using holomorphic properties

We examined two imaging methods, Hilbert microscopy and KK holography, described in terms of holomorphicity and analytic continuation. Consider a sample beam  $S(x)$  scattered from an object and a reference beam  $R(x) = e^{ikx}$  tilted with respect to the detector plane, representing an off-axis configuration, as shown in Fig. 2(a). Hilbert microscopy [46] utilizes an off-axis configuration. The interference pattern  $I$  at the detector is formulated as

$$I = |R + S|^2 = |R|^2 + |S|^2 + 2\text{Re}(R^*S). \quad (9)$$

In Ref. [46], it is assumed that a sample is a phase object with a uniform amplitude to make the  $|S|^2$  a constant. Removing the constant components  $|R|^2$  and  $|S|^2$  leaves  $\text{Re}(R^*S)$ , where the Fourier transform of  $R^*S$  has only positive frequency components under the condition

$$|k| \geq 2\pi(\text{NA})/\lambda. \quad (10)$$

Titchmarsh’s theorem ensures that the Hilbert transform of  $\text{Re}(R^*S)$  provides  $\text{Im}(R^*S)$  and that the sample field  $S$  can be reconstructed from  $\text{Re}(R^*S)$ . The field-retrieval process is shown in Fig. 2(c).

However, unlike the assumption of Ref. [46], even if a sample field has a uniform amplitude, the amplitude of its bandpass-filtered form is not perfectly uniform due to the limited NA of the optical system; thus,  $\mathcal{F}[|S|^2]$  is not completely eliminated by the spatial filtering. Only if  $|R| \gg |S|$ ,  $|S|^2$  can be fully ignored.

The field retrieval of Hilbert microscopy results from the holomorphic properties of a sample field. In contrast, KK holography uses the holomorphic property of the logarithm of the sample field rather than the sample field itself to improve imaging quality. KK holographic imaging corresponds to the 1D phase problem of retrieving the phase of  $R(x) + S(x)$  from the amplitude,  $|R(x) + S(x)|$ .

The holographic imaging method using the KK relations confers the Hilbert transform relation to the real and imaginary parts of the logarithm function of  $R + S$  with  $|R| = 1$ ,

$$\begin{aligned} \log(R + S) &= \log|R + S| + i\mathcal{H}[\log|R + S|] \\ &= \log|R + S| + i\mathcal{H}[\log|R + S|], \end{aligned} \quad (11)$$

when two assumptions are satisfied: (i)  $|R| > |S|$  for all  $x$  and (ii)  $|k| \geq 2\pi(\text{NA})/\lambda$ . These conditions were derived in terms



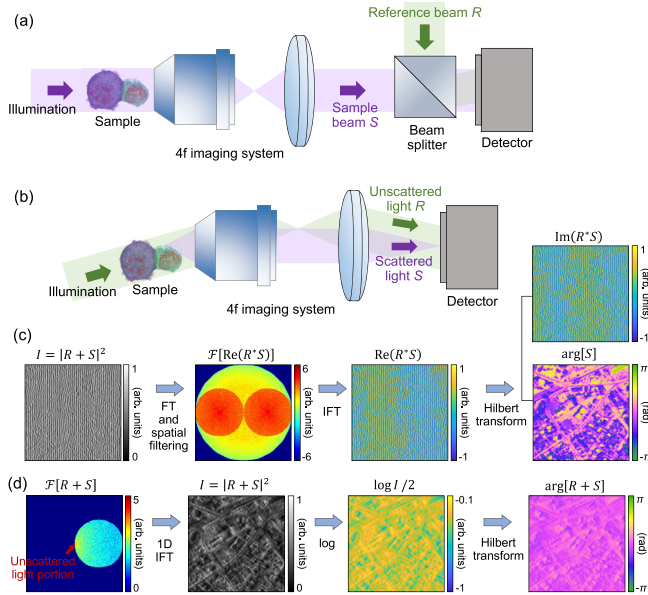


FIG. 2. (a) Schematic diagram of off-axis holography, a setup for Hilbert microscopy. A sample beam is generated by a sample and an illumination, and the interference pattern with a reference beam is acquired from a detector. (b) Schematic diagram of KK holography. The unscattered light from a sample serves as a reference beam. Because  $R + S$  is the same as a sample beam itself, no interference fringe appears on the detector. (c) Field-retrieval procedure in Hilbert microscopy. Spatial filtering of the DC component of an intensity distribution provides the Fourier transform of  $2\text{Re}(R^*S)$ . The Hilbert transform reconstructs  $R^*S$ . (d) Process of the field retrieval in KK holography. The Fourier transform of  $R + S$  is translated so that the Fourier spectrum does not have negative-frequency components. The intensity  $|R + S|^2$  is obtained from a detector. The Hilbert transform of  $\log |R + S|$  renders the phase of  $R + S$  when satisfying the two conditions; the sample field is reconstructed. FT and IFT are the Fourier transform and the inverse Fourier transform, respectively. Images in Fourier space are represented by a log scale.

of complex analysis described in the previous section. Compared with the condition of Hilbert microscopy  $|R| \gg |S|$ , the condition  $|R| > |S|$  is a relaxed requirement.

In the non-interferometric KK holographic imaging [33], the unscattered light takes the role of a reference beam  $R$  [Fig. 2(b)]. The samples that can be imaged are limited to weak-scattering objects due to the condition  $|R| > |S|$ , and the incident angle of the illumination should match the NA of the objective lens, satisfying the condition  $|k| \geq 2\pi(\text{NA})/\lambda$ . Figure 2(d) shows the process of field reconstruction with a Hilbert transform. The intensity distribution of an optical field, whose negative frequencies are suppressed, is measured in a detector.

Intriguingly, Hilbert microscopy and KK holography require similar imaging conditions. Hilbert microscopy can also be considered in the noninterferometric regime [Fig. 2(b)]. Using the same illumination scheme as in noninterferometric KK holography, the same imaging conditions can be reached when using Hilbert microscopy with  $|R| \gg |S|$ . When  $|R|$  is larger than  $|S|$ , the solution given by Hilbert microscopy approaches the field retrieved by KK holography. We

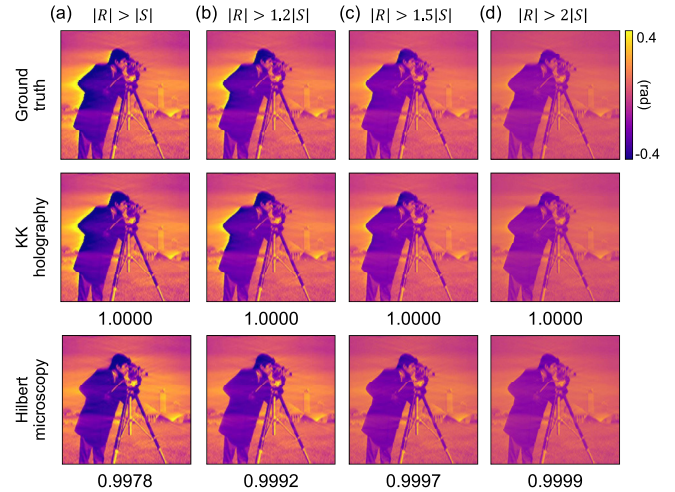


FIG. 3. Comparison of the retrieved phases in KK holography and Hilbert microscopy. (a)–(d) While changing  $|R|$  with respect to  $|S|$ , the solutions for the two methods are observed:  $|R| > |S|$  (a),  $|R| > 1.2|S|$  (b),  $|R| > 1.5|S|$  (c), and  $|R| > 2|S|$  (d). As  $|R|$  becomes larger, the solution of Hilbert microscopy converges to the ground truth and the complex field reconstructed in KK holography. The number below the image is the correlation of the retrieved field with the ground truth.

simulated Hilbert microscopy and KK holography in this situation [Fig. 2(b)] while satisfying the condition of Eq. (10) and by varying the amplitude of the unscattered light, as shown in Fig. 3. If  $|R| > |S|$ , the reconstructed field from KK holography equals the ground truth. Although Hilbert microscopy requires the condition of  $|R| \gg |S|$ , it shows a high correlation with the solution of KK holography even when  $|R|$  is not significantly larger than  $|S|$ . When  $|R| > 2|S|$  is used [Fig. 3(d)], it can be confirmed that the two solutions are almost identical (correlation of 0.9999). Note that  $|R| > a|S|$  implies that  $|R|$  equals the supremum of  $a|S|$ , where  $a$  is a constant.

#### D. Deviation from the conditions of KK holography

If the two conditions invoked in the previous section are satisfied, KK holography provides a correct solution [Fig. 4(a)]. Here, we compare the effects of either of the two conditions being violated. Figs. 4(b)–4(e) show the results obtained by changing the amplitude of the unscattered field, while the condition  $k \leq -C$  holds, where  $C$  is  $2\pi(\text{NA})/\lambda$ , corresponding to 50 pixels. It can be seen that as the intensity of the unscattered field decreases, the phase variation of the complex field increases. Figure 4(b) exhibits a high fidelity because  $|R|$  is the same as the maximum of  $|R| > |S|/2$  so that the number of pixels satisfying  $|R| > |S|$  is still large. In the situation in Fig. 4(d), the retrieved phase is significantly different from the ground truth. In particular, it can be seen that the deviation is larger in the part where the phase changes rapidly.

On the other hand, while the condition  $|R| > |S|$  is maintained, the fidelity is examined by changing the deviation from the condition  $k \leq -C$  [Figs. 4(f)–4(i)].  $k = -C$  is a situation in which the condition is most tightly satisfied, and the retrieved phase is observed while moving the illumination

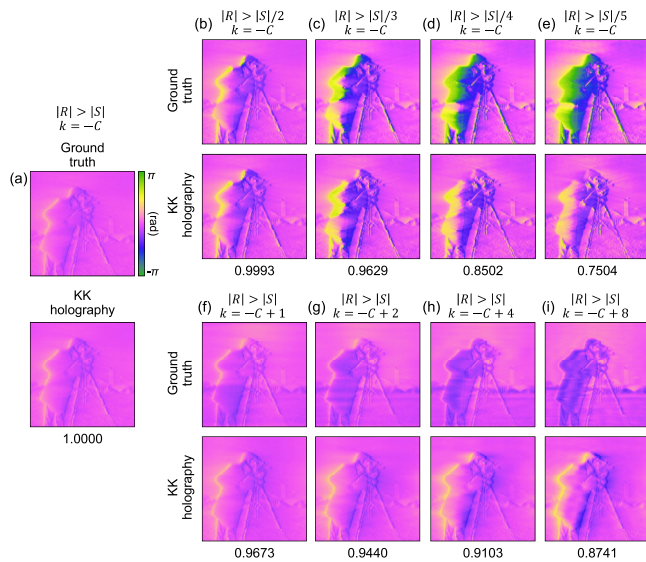


FIG. 4. (a) Reconstructed phase image when the two conditions of KK holography hold. (b)–(i) Reconstructed phase image in the presence of violation for the two conditions with changing the amplitude of the unscattered light (b)–(e) and the number of deviated pixels from  $k = -C$  (f)–(i), where  $C$  is  $2\pi(\text{NA})/\lambda$ . The number below the retrieved phase image means the fidelity of the complex field reconstructed by KK holography.

from a few pixels in Fourier space. One pixel is the inverse of the image size in real space. As expected, it can be seen that the fidelity decreases as the condition is violated. In the case of ground truth, as the number of deviated pixels increases, it approaches the field from normal illumination, so the phase change according to the position becomes less rapid. In contrast, the solution derived by KK holography exhibits a more asymmetric distribution of the phase in the left and right directions, representing an increase in reconstruction error.

We experimentally investigated the effect of deviation from imaging conditions on KK holographic imaging. To clearly inspect the difference in the imaging results of a bead, complex fields obtained from four oblique incident angles were synthesized in Fourier space using a synthetic aperture method [66] to obtain a single-phase image [Fig. 5(a)]. Unless synthetic aperture microscopy is employed, it is difficult to recognize the complete shape of a bead because the spatial frequency distribution of the bead is asymmetrical. We imaged 10- $\mu\text{m}$ -diameter polystyrene beads (RI of 1.5983 at 532 nm, Sigma-Aldrich, 72986-5ML-F) immersed in oil media with different RIs using a conventional off-axis holography setup [67]. Varying the RI of the immersion enables adjustment of the amount of scattering from the sample so that the conditions of KK holography become violated for a low RI of the immersion.

As the RI difference between the bead and medium increases, the phase delay increases, and the intensity of the unscattered light decreases. Figure 5(b) shows the imaging results according to the intensity of the unscattered light. The ground truth was generated using off-axis holography, which accurately reconstructs a light phase. When the RI of the medium is 1.5868, and the phase delay of a bead is

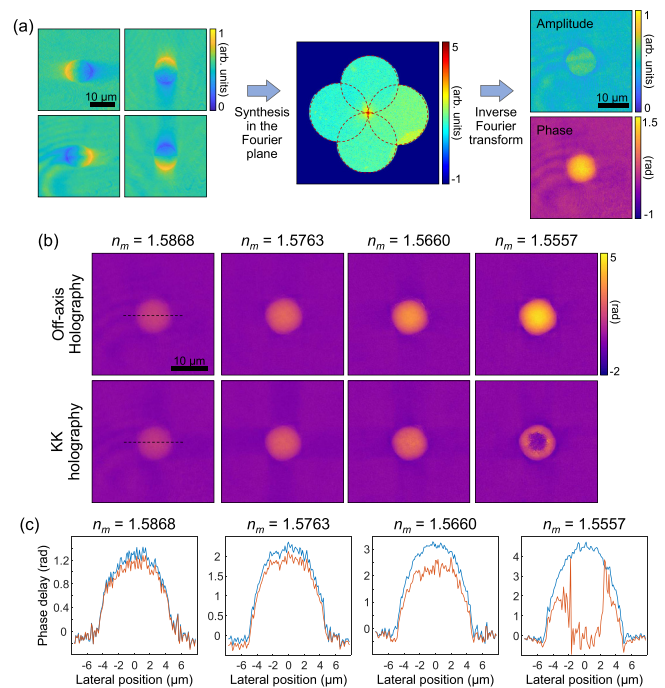


FIG. 5. (a) Reconstruction of a bead image using synthetic aperture microscopy. (Left) Amplitude images of a bead acquired at four oblique incident angles. (Middle) Fourier transform of the four complex fields synthesized in Fourier space. (Right) Amplitude and phase images of a bead obtained by the inverse Fourier transform. (b) Reconstructed phase of beads in media with different RIs using off-axis holography and KK holography. (c) Line profile of the retrieved phase of beads in off-axis holography (blue line) and KK holography (orange line). The dashed line indicates the location where the line profile is obtained. The RI of the medium was obtained at a wavelength of 532 nm.

less than 1.4 rad, KK holography retrieves a phase image similar to the ground truth. In this case, we checked that the intensity of the unscattered light is greater than the intensity of the scattered light, except at a few positions. However, the larger the phase delay of the bead, the greater the difference between the ground truth and the bead image reconstructed by KK holography. This deviation can be viewed quantitatively in Fig. 5(c). For the immersion medium with a medium RI of 1.5660, there was already a noticeable deviation from the ground truth. When the phase delay increases, the phase sharply decreases at the center of the bead imaged with KK holography, which resembles a hole. The error is larger at the center of the bead because the phase delay increases closer to the center; thus, the violation of the assumption  $|R| > |S|$  becomes severe.

It is possible to think quantitatively about the range of a phase delay where the fidelity of KK holography is maintained. For a phase object and normal illumination under the assumption of elastic scattering, the range of the phase delay in which  $|R| > |S|$  holds is up to  $\pi/3$ . This range can be calculated by setting the unscattered and scattered fields to 1 and  $e^{i\theta} - 1$ , respectively, where  $\theta$  is the phase delay (the total field is  $e^{i\theta}$ ) as follows:  $1 > |e^{i\theta} - 1|$ . This phase delay corresponds to the situation with a medium RI of 1.5868. Even

beyond  $\pi/3$ , KK holography seems to give somewhat correct phase values, observing the bead in a medium RI of 1.5763. This is because the limited phase delay  $\pi/3$  is calculated by considering normal illumination. However, in KK holography, the imaging configuration addresses oblique illumination. Assume that the unscattered fields from normal and oblique illuminations are the same, which holds for thin objects. The Fourier coefficient of the scattered field gets smaller the further away from the DC term for most of the samples we are interested in, and the scattered field is cropped by the limited NA of the optical system. This is why it is expected that the amplitude of the scattered field from oblique illumination is generally smaller than that from normal illumination. Thus, the phase-delay range in which  $|R| > |S|$  holds is wider for oblique illumination than for normal illumination; it can be larger than  $\pi/3$ . As a result, KK holographic imaging provides a value similar to the ground truth for a phase delay of  $2\pi/3$ , corresponding to the situation with a medium RI of 1.5763.

### III. DISCUSSION

KK holographic imaging was described by the relationship between a holomorphic field and its zeros. It is important to know the position of the zeros because one can fully determine a holomorphic complex field using its zeros and the Hadamard factorization theorem [49,68].

Interestingly, the problem of eliminating zeros is also associated with minimum phase systems in the field of signals and systems [69,70]. A minimum phase system has the minimum group delay for a given signal magnitude [71]. The group delay is represented by the phase response of a system for frequency. In minimum phase systems, the characteristics of stability and causality can be utilized [72]. Also, because minimum phase systems provide a direct relationship between the magnitude and phase as a Hilbert transform, a received signal can be reconstructed from a detector insensitive to phase [70].

One important problem to be addressed in imaging systems is how the signal-to-noise ratio (SNR) affects imaging capability [73,74]. The accuracy in KK holographic imaging can be evaluated using the boundedness of the Hilbert transform because the KK relations correspond to the directional Hilbert transform. In Ref. [33], it is shown that the root-mean-square (rms) of the phase error is less than or equal to the rms of

$\log(1 + N/I_0)/2$ , where  $N$  is added noise, and  $I_0$  is a noise-free intensity image. A more profound discussion of noise characteristics when using a Hilbert transform can be found in Ref. [75]. In addition, for most samples for which the KK holography conditions hold, the magnitude of the Fourier coefficient decreases as spatial frequency increases, so the SNR is also reduced with increasing spatial frequency, resulting in a diminution of image resolution [73]. We anticipate that the SNR for transmitting high spatial frequency can be raised by optimizing the pupil function in the Fourier plane [74].

Although this study focuses on using the relation of a Hilbert transform by eliminating zeros, it is also possible to infer the shape of a complex field by directly finding zeros [76,77]. Moreover, because the configuration in which the conditions of KK holographic imaging are violated is the same as the situation in which zeros exist in the UHP, the deviation can be interpreted with the derived complex zeros [38]. However, in the 1D phase problem, it is necessary to create additional conditions for the zeros because there is ambiguity in zeros when only a single-magnitude distribution of a complex field is given.

Due to its quantitative and label-free imaging capability, QPI has been utilized in various fields, with emphasis on the interpretation of QPI data using machine-learning approaches [78–83]. However, the complication in constructing interferometric microscopy has hindered wider applications. We envision the present method—QPI via the holomorphic property of complex optical fields—would serve as an important basis for a comprehensive understanding of phase retrieval problems in holographic imaging as well as expand the applicability of QPI.

The implementation code and data used in this work are available in Ref. [84].

### ACKNOWLEDGMENTS

This work was supported by National Research Foundation of Korea (2015R1A3A2066550, 2022M3H4A1A02074314), Institute of Information & communications Technology Planning & Evaluation (IITP; 2021-0-00745) grant funded by the Korea government (MSIT), KAIST Institute of Technology Value Creation, Industry Liaison Center (G-CORE Project) grant funded by MSIT (N11230131).

- 
- [1] P. Memmolo, L. Miccio, M. Paturzo, G. Di Caprio, G. Coppola, P. A. Netti, and P. Ferraro, Recent advances in holographic 3D particle tracking, *Adv. Opt. Photonics* **7**, 713 (2015).
  - [2] S. Grilli, S. Coppola, V. Vespini, F. Merola, A. Finizio, and P. Ferraro, 3D lithography by rapid curing of the liquid instabilities at nanoscale, *Proc. Natl. Acad. Sci.* **108**, 15106 (2011).
  - [3] S. Y. Choi, J. Oh, J. Jung, Y. Park, and S. Y. Lee, Three-dimensional label-free visualization and quantification of polyhydroxyalkanoates in individual bacterial cell in its native state, *Proc. Natl. Acad. Sci.* **118**, e2103956118 (2021).
  - [4] T.-W. Su, L. Xue, and A. Ozcan, High-throughput lens-free 3D tracking of human sperms reveals rare statistics of helical trajectories, *Proc. Natl. Acad. Sci.* **109**, 16018 (2012).
  - [5] B. Kemper, D. D. Carl, J. Schnekenburger, I. Bredebusch, M. Schäfer, W. Domschke, and G. von Bally, Investigation of living pancreas tumor cells by digital holographic microscopy, *J. Biomed. Opt.* **11**, 034005 (2006).
  - [6] J. van der Horst, A. K. Trull, and J. Kalkman, Deep-tissue label-free quantitative optical tomography, *Optica* **7**, 1682 (2020).
  - [7] W. Bishara, H. Zhu, and A. Ozcan, Holographic opto-fluidic microscopy, *Opt. Express* **18**, 27499 (2010).
  - [8] L. Miccio, P. Memmolo, F. Merola, P. Netti, and P. Ferraro, Red blood cell as an adaptive optofluidic microlens, *Nat. Commun.* **6**, 1 (2015).



- [9] Y. Fainman, D. Psaltis, and C. Yang, *Optofluidics: Fundamentals, Devices, and Applications* (McGraw-Hill Education, New York, 2010).
- [10] F. Merola, P. Memmolo, L. Miccio, R. Savoia, M. Mugnano, A. Fontana, G. D'Ippolito, A. Sardo, A. Iolascon, A. Gambale, and P. Ferraro, Tomographic flow cytometry by digital holography, *Light: Sci. Appl.* **6**, e16241 (2017).
- [11] B. Bhaduri, C. Edwards, H. Pham, R. Zhou, T. H. Nguyen, L. L. Goddard, and G. Popescu, Diffraction phase microscopy: Principles and applications in materials and life sciences, *Adv. Opt. Photonics* **6**, 57 (2014).
- [12] G. Taylor, The phase problem, *Acta Crystallogr., Sect. D: Biol. Crystallogr.* **59**, 1881 (2003).
- [13] T. I. Kuznetsova, On the phase retrieval problem in optics, *Sov. Phys. Usp.* **31**, 364 (1988).
- [14] J. R. Fienup, Phase retrieval algorithms: A comparison, *Appl. Opt.* **21**, 2758 (1982).
- [15] Y. Park, C. Depeursinge, and G. Popescu, Quantitative phase imaging in biomedicine, *Nat. Photonics* **12**, 578 (2018).
- [16] B. Kemper, A. Vollmer, G. von Bally, C. E. Rommel, and J. Schnekenburger, Simplified approach for quantitative digital holographic phase contrast imaging of living cells, *J. Biomed. Opt.* **16**, 026014 (2011).
- [17] M. Lee, E. Lee, J. Jung, H. Yu, K. Kim, J. Yoon, S. Lee, Y. Jeong, and Y. Park, Label-free optical quantification of structural alterations in Alzheimer's disease, *Sci. Rep.* **6**, 1 (2016).
- [18] K. Kim, W. S. Park, S. Na, S. Kim, T. Kim, W. Do Heo, and Y. Park, Correlative three-dimensional fluorescence and refractive index tomography: Bridging the gap between molecular specificity and quantitative bioimaging, *Biomed. Opt. express* **8**, 5688 (2017).
- [19] M. Esposito, C. Fang, K. C. Cook, N. Park, Y. Wei, C. Spadazzi, D. Bracha, R. T. Gunaratna, G. Laevsky, and C. J. DeCoste, TGF- $\beta$ -induced DACT1 biomolecular condensates repress Wnt signalling to promote bone metastasis, *Nat. Cell Biol.* **23**, 257 (2021).
- [20] B. Hoenders, On the solution of the phase retrieval problem, *J. Math. Phys.* **16**, 1719 (1975).
- [21] J. Wood, M. A. Fiddy, and R. Burge, Phase retrieval using two intensity measurements in the complex plane, *Opt. Lett.* **6**, 514 (1981).
- [22] R. Burge, M. Fiddy, A. Greenaway, and G. Ross, The phase problem, *Proc. R. Soc. London, Ser. A: Math. Phys. Sci.* **350**, 191 (1976).
- [23] G. Zheng, R. Horstmeyer, and C. Yang, Wide-field, high-resolution Fourier ptychographic microscopy, *Nat. Photonics* **7**, 739 (2013).
- [24] J. R. Fienup, Reconstruction of a complex-valued object from the modulus of its Fourier transform using a support constraint, *JOSA A* **4**, 118 (1987).
- [25] G.-z. Yang, B.-z. Dong, B.-y. Gu, J.-y. Zhuang, and O. K. Ersoy, Gerchberg-Saxton and Yang-Gu algorithms for phase retrieval in a nonunitary transform system: A comparison, *Appl. Opt.* **33**, 209 (1994).
- [26] E. Cuche, P. Marquet, and C. Depeursinge, Spatial filtering for zero-order and twin-image elimination in digital off-axis holography, *Appl. Opt.* **39**, 4070 (2000).
- [27] I. Yamaguchi, Phase-shifting digital holography, in *Digital Holography and Three-Dimensional Display* (Springer, Boston, 2006), pp. 145–171.
- [28] D. Paganin and K. A. Nugent, Noninterferometric Phase Imaging with Partially Coherent Light, *Phys. Rev. Lett.* **80**, 2586 (1998).
- [29] D. Paganin and K. A. Nugent, Noninterferometric phase determination, in *Advances in Imaging and Electron Physics* (Elsevier, Amsterdam, 2001), pp. 85–127.
- [30] K. Chalasincka-Macukow and H. Arsenault, Fast iterative solution to exact equations for the two-dimensional phase-retrieval problem, *JOSA A* **2**, 46 (1985).
- [31] L. Waller, Y. Luo, S. Y. Yang, and G. Barbastathis, Transport of intensity phase imaging in a volume holographic microscope, *Opt. Lett.* **35**, 2961 (2010).
- [32] C. Zuo, J. Li, J. Sun, Y. Fan, J. Zhang, L. Lu, R. Zhang, B. Wang, L. Huang, and Q. Chen, Transport of intensity equation: A tutorial, *Opt. Lasers Eng.* **135**, 106187 (2020).
- [33] Y. Baek and Y. Park, Intensity-based holographic imaging via space-domain Kramers-Kronig relations, *Nat. Photonics* **15**, 354 (2021).
- [34] Y. Baek, K. Lee, S. Shin, and Y. Park, Kramers-Kronig holographic imaging for high-space-bandwidth product, *Optica* **6**, 45 (2019).
- [35] N. Nakajima and T. Asakura, Two-dimensional phase retrieval using the logarithmic Hilbert transform and the estimation technique of zero information, *J. Phys. D: Appl. Phys.* **19**, 319 (1986).
- [36] A. Greenaway, Proposal for phase recovery from a single intensity distribution, *Opt. Lett.* **1**, 10 (1977).
- [37] N. Nakajima and T. Asakura, A new approach to two-dimensional phase retrieval, *Optica Acta: Int. J. Opt.* **32**, 647 (1985).
- [38] M. Fiddy and A. Greenaway, Phase retrieval using zero information, *Opt. Commun.* **29**, 270 (1979).
- [39] C. Shen, M. Liang, A. Pan, and C. Yang, Non-iterative complex wave-field reconstruction based on Kramers-Kronig relations, *Photonics Res.* **9**, 1003 (2021).
- [40] Y. Li, C. Shen, J. Tan, X. Wen, M. Sun, G. Huang, S. Liu, and Z. Liu, Fast quantitative phase imaging based on Kramers-Kronig relations in space domain, *Opt. Express* **29**, 41067 (2021).
- [41] C. Lee, Y. Baek, H. Hugonnet, and Y. Park, Single-shot wide-field topography measurement using spectrally multiplexed reflection intensity holography via space-domain Kramers-Kronig relations, *Opt. Lett.* **47**, 1025 (2022).
- [42] Z. Huang and L. Cao, High bandwidth-utilization digital holographic multiplexing: An approach using Kramers-Kronig relations, *Adv. Photonics Res.* **3**, 2100273 (2022).
- [43] Y. Li, X. Wen, M. Sun, X. Zhou, Y. Ji, G. Huang, K. Zhou, S. Liu, and Z. Liu, Spectrum sampling optimization for quantitative phase imaging based on Kramers-Kronig relations, *Opt. Lett.* **47**, 2786 (2022).
- [44] R. Lane, W. Fright, and R. Bates, Direct phase retrieval, *IEEE Trans. Acoust. Speech Signal Process.* **35**, 520 (1987).
- [45] M. Scivier and M. Fiddy, Phase ambiguities and the zeros of multidimensional band-limited functions, *JOSA A* **2**, 693 (1985).
- [46] T. Ikeda, G. Popescu, R. R. Dasari, and M. S. Feld, Hilbert phase microscopy for investigating fast dynamics in transparent systems, *Opt. Lett.* **30**, 1165 (2005).
- [47] E. M. Stein and R. Shakarchi, *Complex Analysis* (Princeton University Press, Princeton, New Jersey, 2010).

- [48] R. E. A. C. Paley and N. Wiener, *Fourier Transforms in the Complex Domain* (American Mathematical Society, Providence, RI, 1934).
- [49] R. P. Boas, *Entire Functions* (Academic Press, Cambridge, 2011).
- [50] E. Hille and J. D. Tamarkin, On a theorem of Paley and Wiener, *Ann. Math.* **34**, 606 (1933).
- [51] A. Walther, The question of phase retrieval in optics, *Optica Acta: Int. J. Opt.* **10**, 41 (1963).
- [52] R. A. Silverman, *Complex Analysis with Applications* (Courier Corporation, North Chelmsford, MA, 1984).
- [53] S. Lang, *Complex Analysis* (Springer Science & Business Media, Berlin, 2003).
- [54] J. Franklin, Analytic continuation by the fast Fourier transform, *SIAM J. Sci. Stat. Comput.* **11**, 112 (1990).
- [55] S. Wadaka and T. Sato, Superresolution in incoherent imaging system, *JOSA* **65**, 354 (1975).
- [56] H. A. Kramers, La diffusion de la lumiere par les atomes, in *Atti Cong. Intern. Fisica (Transactions of Volta Centenary Congress)* (Como, Lombardy, Italy, 1927), pp. 545–557.
- [57] K. R. Waters, J. Mobley, and J. G. Miller, Causality-imposed (Kramers-Kronig) relationships between attenuation and dispersion, *IEEE Trans. Ultrason. Ferroelectr. Freq. Control* **52**, 822 (2005).
- [58] M. Sharnoff, Validity conditions for the Kramers-Kronig relations, *Am. J. Phys.* **32**, 40 (1964).
- [59] E. C. Titchmarsh, The zeros of certain integral functions, *Proc. London Math. Soc.* **s2**, 283 (1926).
- [60] L. V. Ahlfors, *Complex analysis: An Introduction to the Theory of Analytic Functions of One Complex Variable* (New York, 1953), p. 177.
- [61] D. Sarason, *Complex Function Theory* (American Mathematical Society, Providence, RI, 2007).
- [62] A. Zygmund, *Trigonometric Series* (Cambridge University Press, Cambridge, 2002).
- [63] H. Hedenmalm, A factorization theorem for square area-integrable analytic functions, *Journal für die reine und angewandte Mathematik* **422**, 45 (1991).
- [64] J. Mashreghi, Hilbert transform of  $\log|f|$ , *Proc. Am. Math. Soc.* **130**, 683 (2002).
- [65] T. Boland, R. Naus, and P. Zwamborn, Phase response reconstruction for non-minimum phase systems using frequency-domain magnitude values, *IET Sci., Meas. Technol.* **15**, 619 (2021).
- [66] C. Zheng, D. Jin, Y. He, H. Lin, J. Hu, Z. Yaqoob, P. T. So, and R. Zhou, High spatial and temporal resolution synthetic aperture phase microscopy, *Adv. Photonics* **2**, 065002 (2020).
- [67] J. Oh, J. S. Ryu, M. Lee, J. Jung, S. Han, H. J. Chung, and Y. Park, Three-dimensional label-free observation of individual bacteria upon antibiotic treatment using optical diffraction tomography, *Biomed. Opt. Express* **11**, 1257 (2020).
- [68] L. de Branges, New and old problems for entire functions, *Bull. Am. Math. Soc.* **70**, 214 (1964).
- [69] P. Dang and T. Qian, Analytic phase derivatives, all-pass filters and signals of minimum phase, *IEEE Trans. Signal Process.* **59**, 4708 (2011).
- [70] A. Mecozzi, A necessary and sufficient condition for minimum phase and implications for phase retrieval, [arXiv:1606.04861](https://arxiv.org/abs/1606.04861) (2016).
- [71] S. Hashemgeloogherdi and M. F. Bocko, Invertibility of acoustic systems: An intuitive physics-based model of minimum phase behavior, *Proc. Mtgs. Acoust.* **23**, 055002 (2015).
- [72] F. F. Li and T. J. Cox, *Digital Signal Processing in Audio and Acoustical Engineering* (CRC Press, Boca Raton, FL, 2019).
- [73] W. Adams, A. Ghoshroy, and D. Ö. Güney, Incoherent Active Convolved Illumination Enhances the Signal-to-Noise Ratio for Shot Noise: Experimental Evidence, *Phys. Rev. Appl.* **18**, 064080 (2022).
- [74] J. Becker, T. Deguchi, A. Jügler, R. Förster, U. Hübner, J. Ries, and R. Heintzmann, Better than a lens? Increasing the signal-to-noise ratio through pupil splitting, *Optica* **10**, 308 (2023).
- [75] P. Pavliček and V. Svak, Noise properties of Hilbert transform evaluation, *Meas. Sci. Technol.* **26**, 085207 (2015).
- [76] A. Noushin, M. Fiddy, and J. Graham-Eagle, Some new findings on the zeros of band-limited functions, *JOSA A* **16**, 1857 (1999).
- [77] J. Wood, T. Hall, and M. Fiddy, A comparison study of some computational methods for locating the zeros of entire functions, *Optica Acta: Int. J. Opt.* **30**, 511 (1983).
- [78] Y. Jo, H. Cho, S. Y. Lee, G. Choi, G. Kim, H.-s. Min, and Y. Park, Quantitative phase imaging and artificial intelligence: A review, *IEEE J. Sel. Top. Quantum Electron.* **25**, 1 (2018).
- [79] S. K. Mirsky, I. Barnea, M. Levi, H. Greenspan, and N. T. Shaked, Automated analysis of individual sperm cells using stain-free interferometric phase microscopy and machine learning, *Cytometry Part A* **91**, 893 (2017).
- [80] M. E. Kandel, Y. R. He, Y. J. Lee, T. H.-Y. Chen, K. M. Sullivan, O. Aydin, M. T. A. Saif, H. Kong, N. Sobh, and G. Popescu, Phase imaging with computational specificity (PICS) for measuring dry mass changes in sub-cellular compartments, *Nat. Commun.* **11**, 1 (2020).
- [81] M. Lee, Y.-H. Lee, J. Song, G. Kim, Y. Jo, H. Min, C. H. Kim, and Y. Park, Deep-learning-based three-dimensional label-free tracking and analysis of immunological synapses of CAR-T cells, *Elife* **9**, e49023 (2020).
- [82] Y. Jo, H. Cho, W. S. Park, G. Kim, D. Ryu, Y. S. Kim, M. Lee, S. Park, M. J. Lee, and H. Joo, Label-free multiplexed microtomography of endogenous subcellular dynamics using generalizable deep learning, *Nat. Cell Biol.* **23**, 1329 (2021).
- [83] G. Kim, D. Ahn, M. Kang, J. Park, D. Ryu, Y. Jo, J. Song, J. S. Ryu, G. Choi, and H. J. Chung, Rapid species identification of pathogenic bacteria from a minute quantity exploiting three-dimensional quantitative phase imaging and artificial neural network, *Light: Sci. Appl.* **11**, 1 (2022).
- [84] J. Oh, H. Hugonnet, and Y. Park, Quantitative phase imaging via the holomorphic property of complex optical fields, <https://github.com/BMOLKAIST/Holomorphic-complex-field-2022>.